Electronic Supplementary Material (ESI) for Dalton Transactions.

<Electronic Supplementary Information>

Formation Procedure of Trimetallic Coordination Cages for Nitrate Encapsulation: Transformation of Kinetic into Thermodynamic Products

Sangwoo Lim, Heehun Moon, Dongwon Kim, and Ok-Sang Jung*

Department of Chemistry, Pusan National University, Busan 46241, Republic of Korea Fax: (+82) 51-5163522;

Tel: (+82) 51-5103240; E-mail: oksjung@pusan.ac.kr

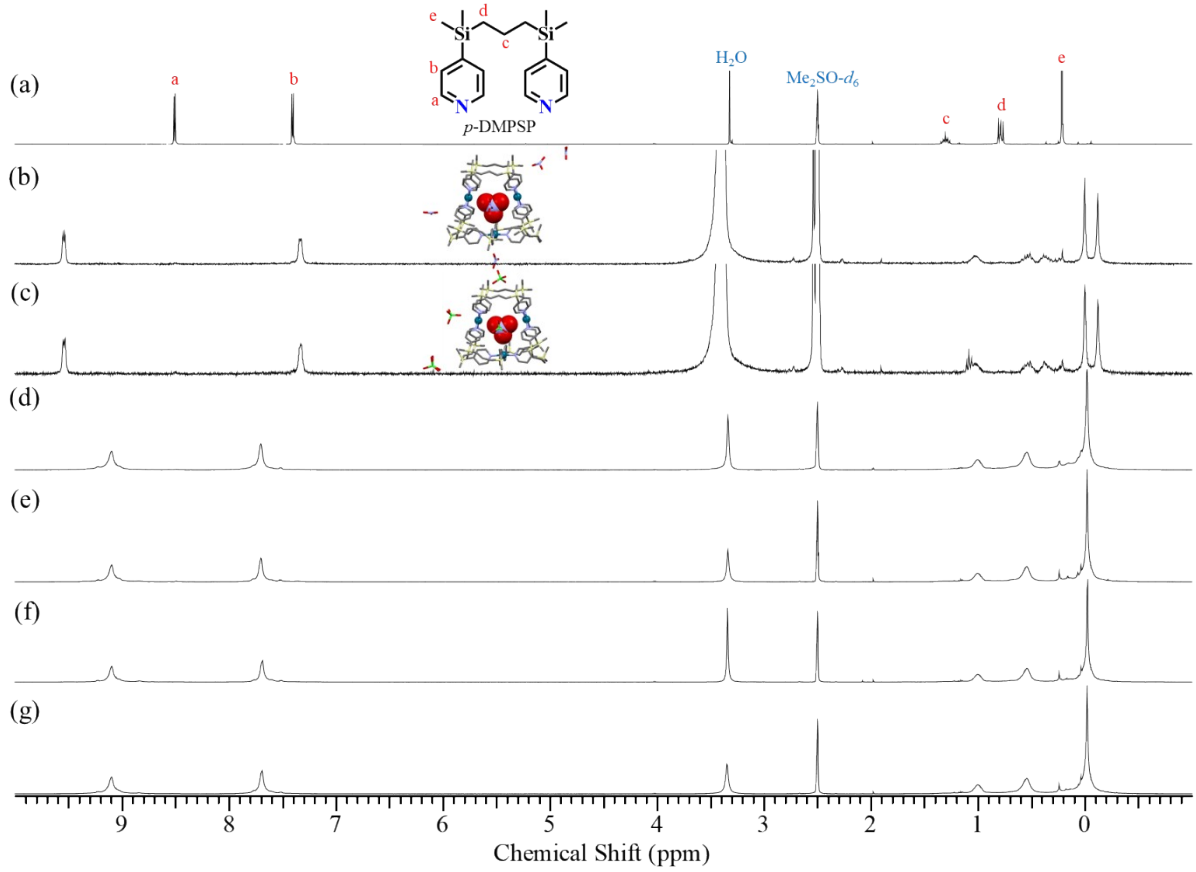

Fig. S1 ^{1}H NMR Spectra for L (a), $[(NO_3)@Pd_3L_6](NO_3)_5{\cdot}2Me_2SO$ (b), $[(NO_3)@Pd_3L_6](ClO_4)_5{\cdot}5Me_2SO$ (c), $[PdL_2](BF_4)_2$ (d), $[PdL_2](ClO_4)_2$ (e), $[PdL_2](PF_6)_2$ (f), and $[PdL_2](CF_3SO_3)_2$ (g) in Me_2SO-d_6.

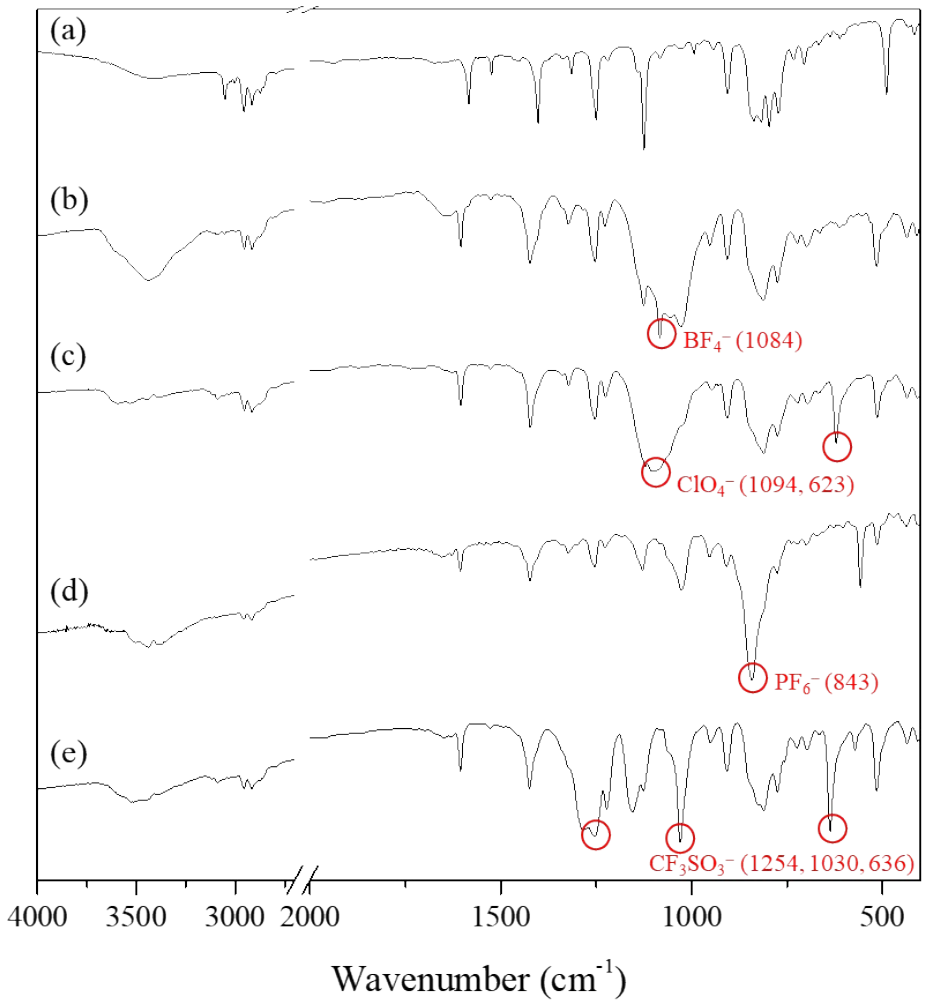

Fig. S2 IR spectra of L (a), $[PdL_2](BF_4)_2$ (b), $[PdL_2](ClO_4)_2$ (c), $[PdL_2](PF_6)_2$ (d), and $[PdL_2](CF_3SO_3)_2$ (e).

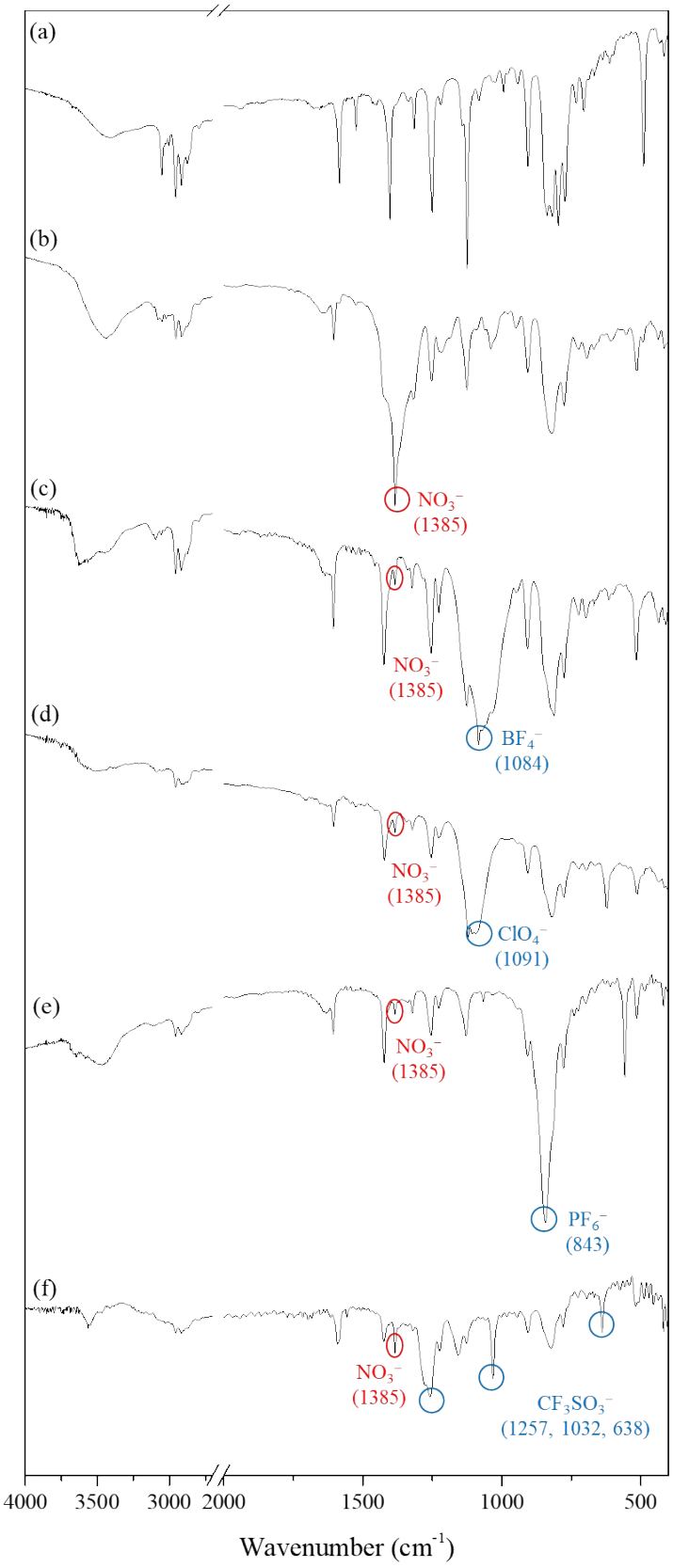

Fig. S3 IR spectra of L (a), $[(NO_3)@Pd_3L_6](NO_3)_5{\cdot}2Me_2SO$ (b), and $[(NO_3)@Pd_3L_6](X)_5$ *via* anion exchange of $[(NO_3)@Pd_3L_6](NO_3)_5{\cdot}2Me_2SO$ with BF_4^- (c), ClO_4^- (d), PF_6^- (e), and $CF_3SO_3^-$ (f).

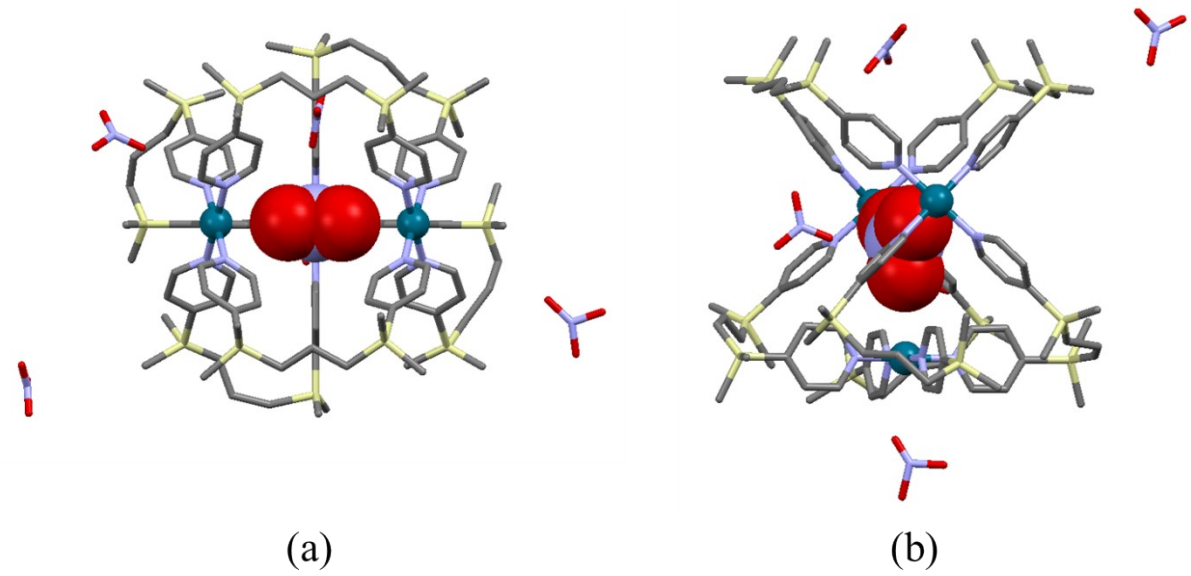

Fig. S4 Crystal structures of $[(NO_3)@Pd_3L_6](NO_3)_5 \cdot 2Me_2SO$ with top view (a) and side view (b).

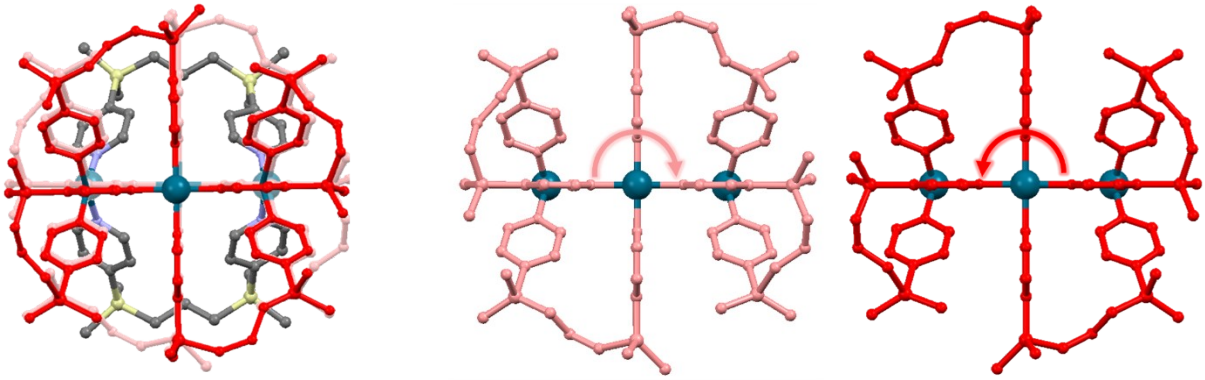

Fig. S5 Crystal structures of $[(NO_3)@Pd_3L_6](NO_3)_5 \cdot 2Me_2SO$ designating the disordered ligands (a): four red ligands. Its separated *P*-helical cage (b), *M*-helical cage (c).

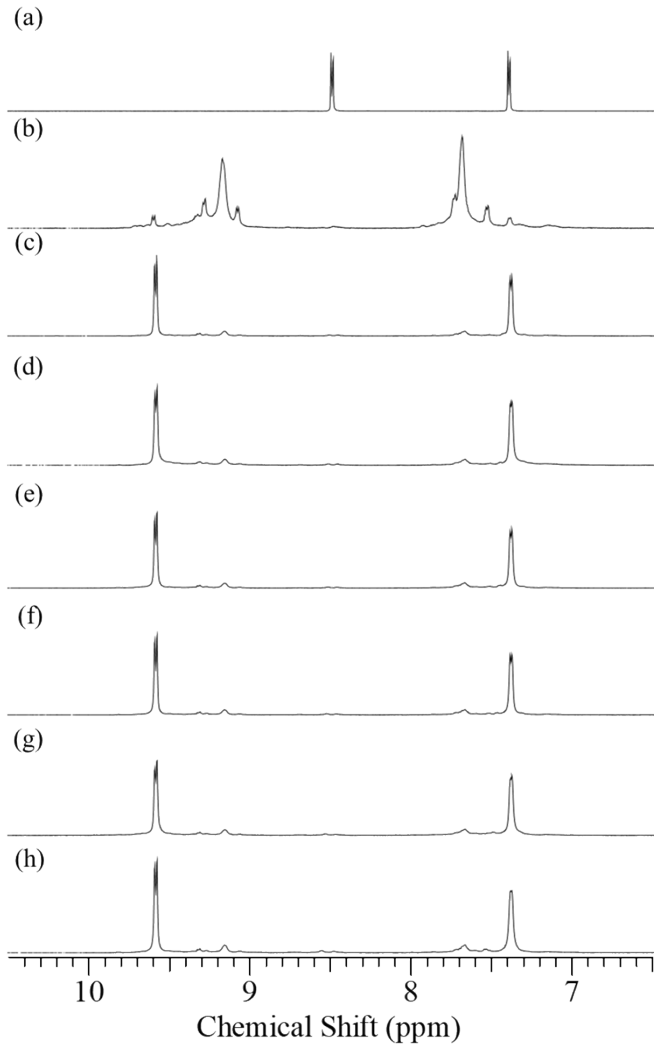

Fig. S6 ^{1}H NMR spectra of L (a), reaction of $Pd(NO_3)_2$ with L at 90 °C for 0 min (b), 10 min (c), 30 min (d), 1 h (e), 2 h (f), 4 h (g), and 12 h (h).

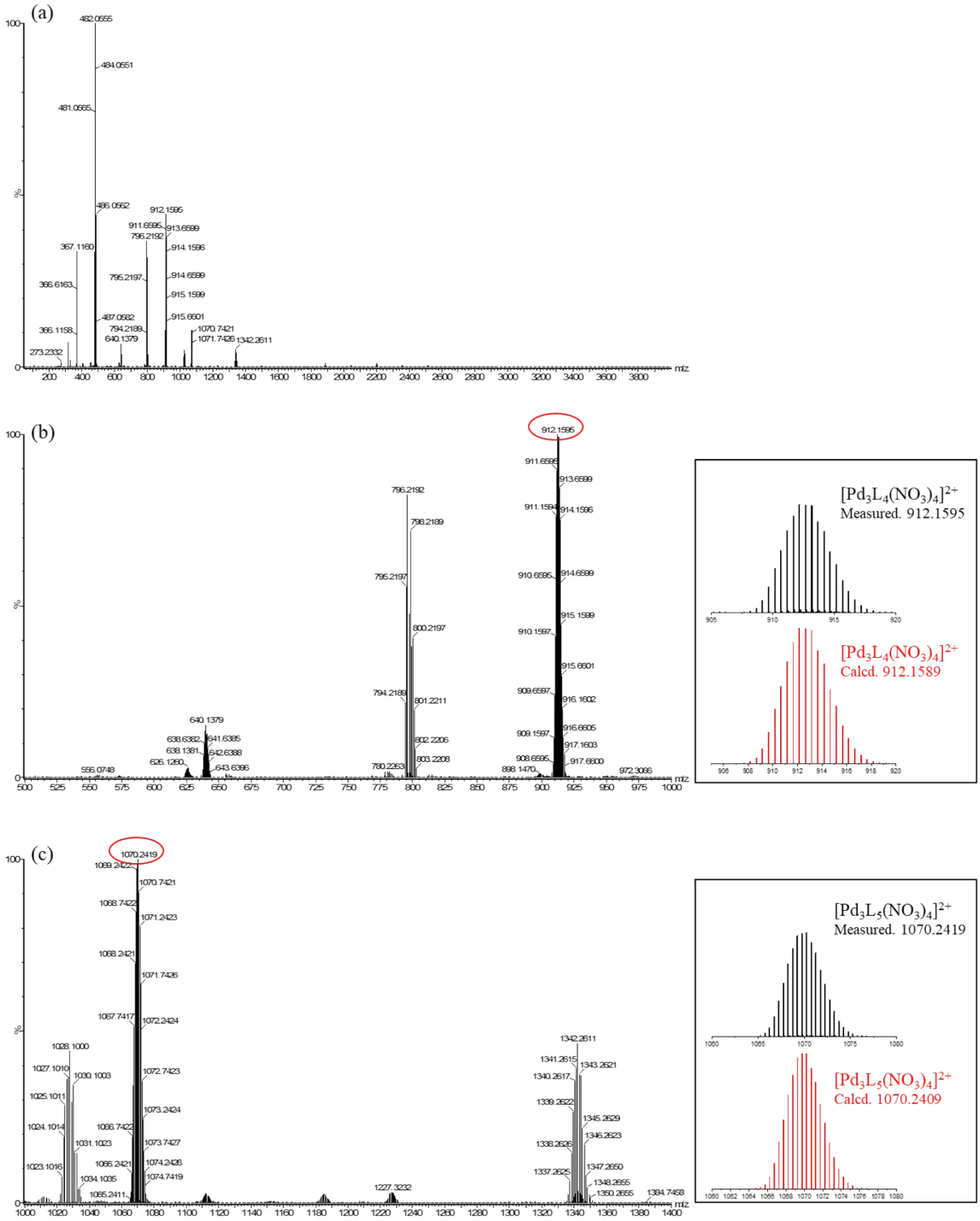

Fig. S7 ESI-TOF-MS data of $[(NO_3)@Pd_3L_6](NO_3)_5{\cdot}2Me_2SO$. m/z range 50-4000 (a), m/z range 500-1000 (b), and m/z range 1000-1400 (c). m/z for $[Pd_3L_4(NO_3)_4]^{2+}$ = 912.1595, $[Pd_3L_5(NO_3)_4]^{+}$ = 1070.2419

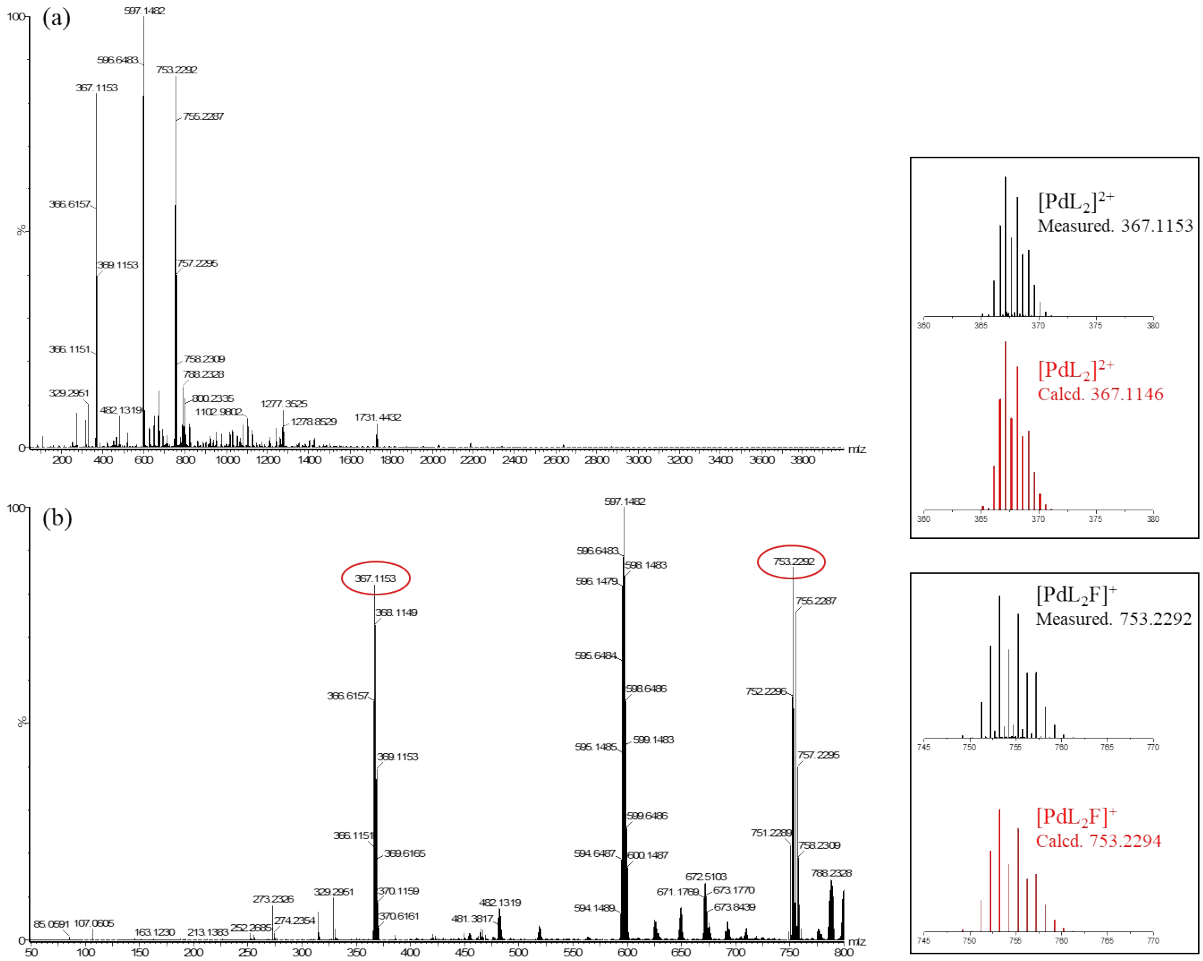

Fig. S8 ESI-TOF-MS data of $[PdL_2](BF_4)_2$. m/z range 50-4000 (a), and m/z range 50-800 (b). m/z for $[PdL_2]^{2+}$ = 367.1153, $[PdL_2]F^{+}$ = 753.2292

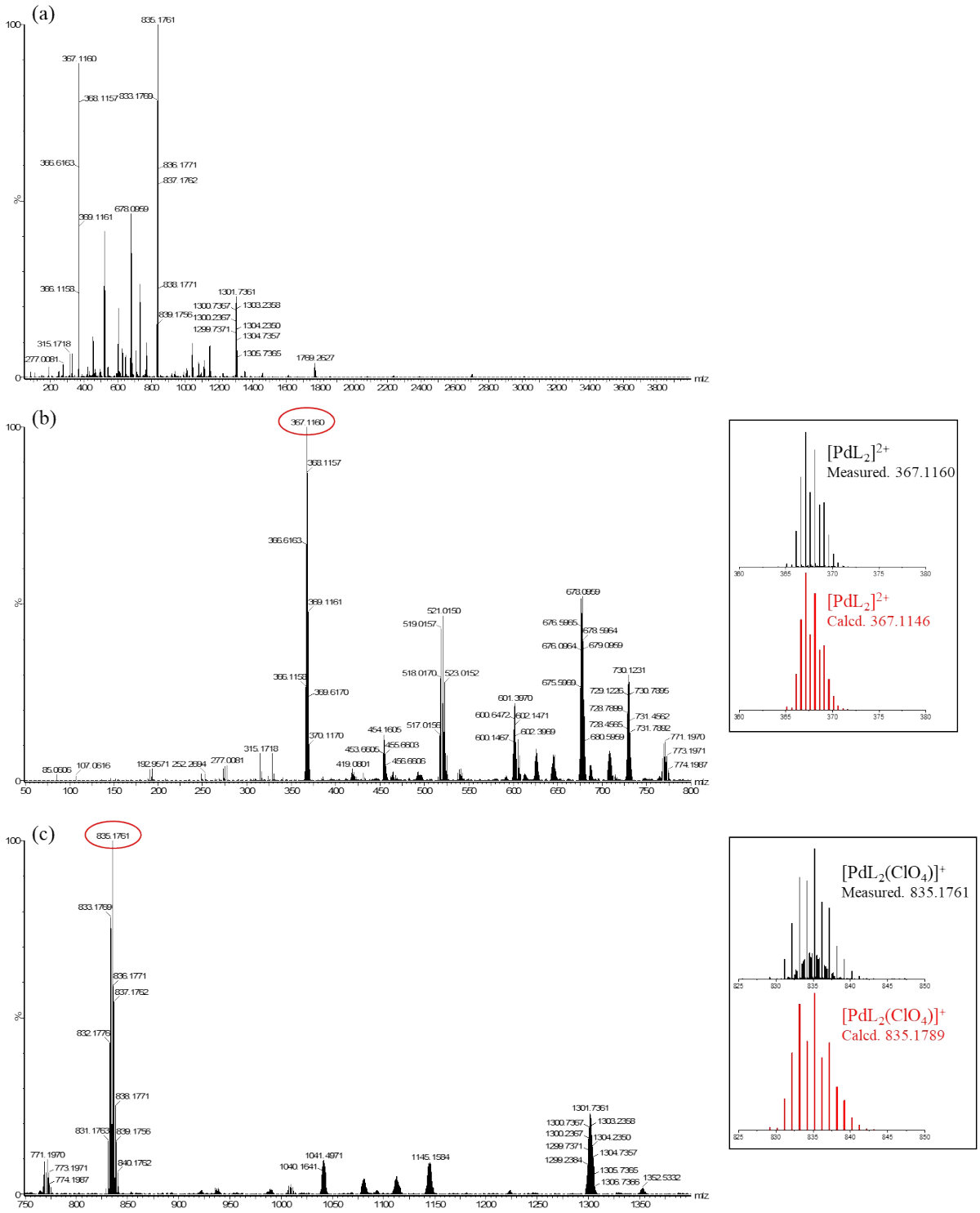

Fig. S9 ESI-TOF-MS data of $[PdL_2](ClO_4)_2$. m/z range 50-4000 (a), m/z range 50-800 (b), and m/z range 750-1400 (c). m/z for $[PdL_2]^{2+}$ = 367.1160, $[PdL_2](ClO_4)^{+}$ = 835.1761

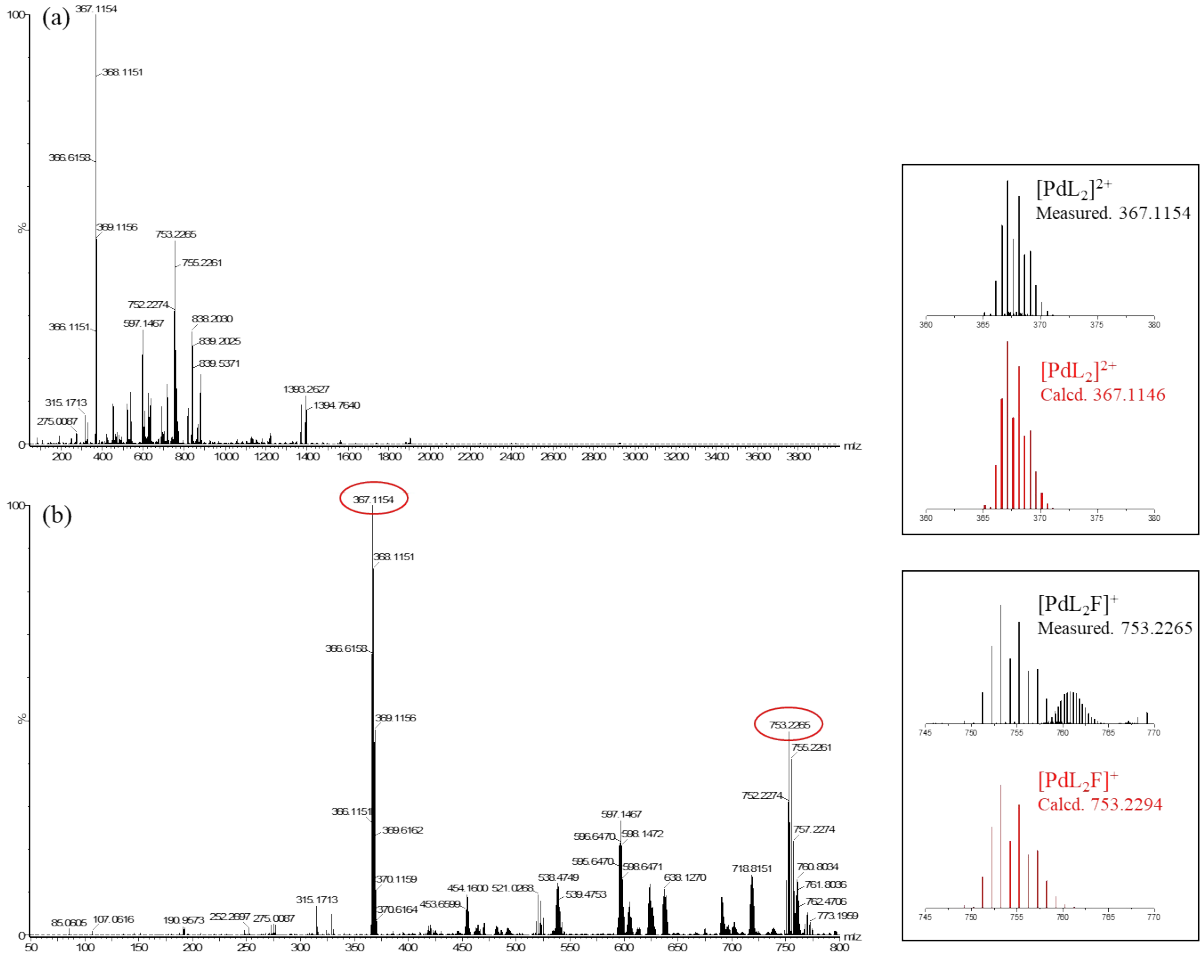

Fig. S10 ESI-TOF-MS data of $[PdL_2](PF_6)_2$. m/z range 50-4000 (a), and m/z range 50-800 (b). m/z for $[PdL_2]^{2+}$ = 367.1154, $[PdL_2]F^{+}$ = 753.2265

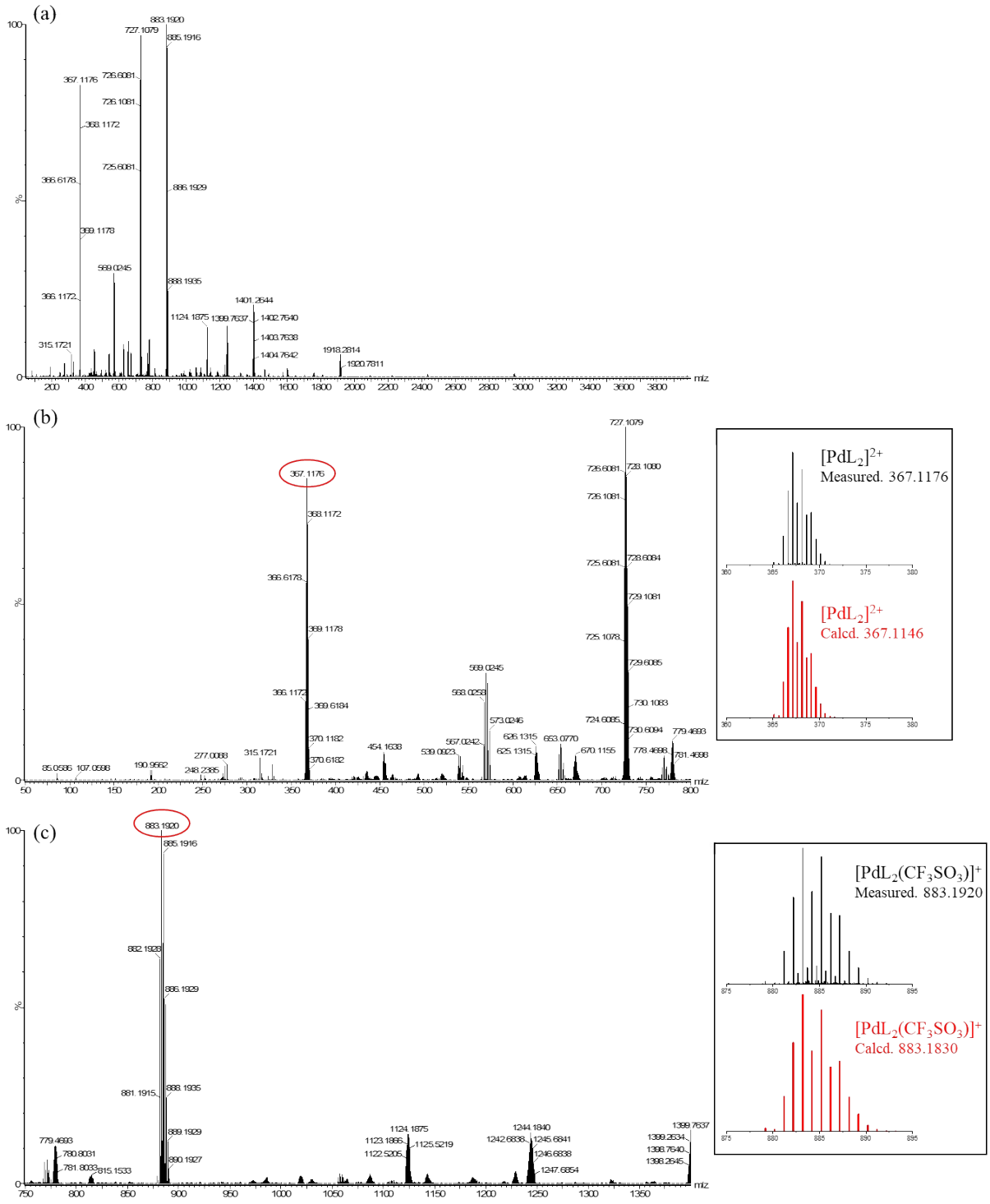

Fig. S11 ESI-TOF-MS data of $[PdL_2](CF_3SO_3)_2$. m/z range 50-4000 (a), m/z range 50-800 (b), and m/z range 750-1400 (c). m/z for $[PdL_2]^{2+}$ = 367.1176, $[PdL_2](ClO_4)^{+}$ = 883.1920

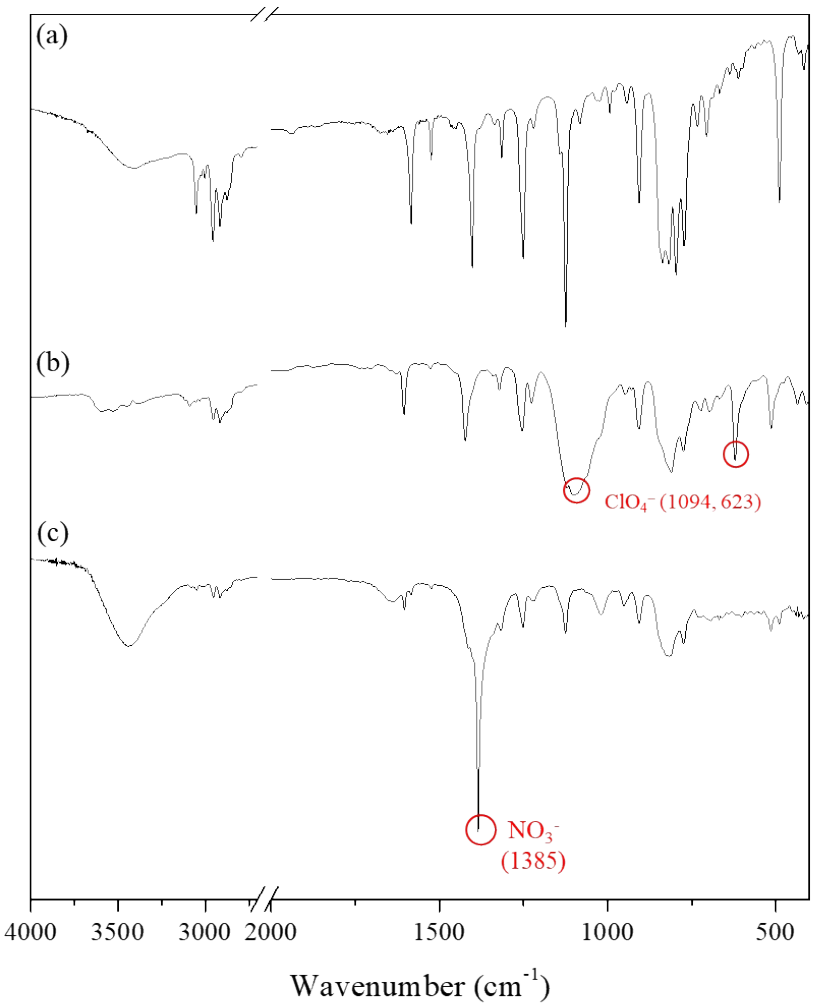

Fig. S12 IR spectra of L (a), $[PdL_2](ClO_4)_2$ (b), and $[(NO_3)@Pd_3L_6](NO_3)_5$ *via* anion exchange of $[PdL_2](ClO_4)_2$ with NO_3^- (c).